Available online at www.sciencedirect.com
ScienceDirect
Journal of the European Ceramic Society 27 (2007) 19–25
www.elsevier.com/locate/jeurceramsoc

Halos mechanism in stabilizing of colloidal suspensions: Nanoparticle weight fraction and pH effects

H. Karimian, A.A. Babaluo *

Research Center for Polymeric Materials, Sahand University of Technology, P.O. Box 51335/1996, Tabriz, Iran

Received 9 November 2005; received in revised form 22 April 2006; accepted 10 May 2006
Available online 22 August 2006

Abstract

Nanoparticle halo is a novel method that stabilizes colloidal suspensions with high efficiency compared to conventional methods. But, up to now few articles have been published on the stabilization mechanism of this method. This article investigates the dispersion behavior of colloidal Al_2O_3 aqueous suspensions in the presence of highly charged CeO_2 nanoparticles and the effect of two key parameters; the ceria nanoparticle concentration and pH on the stability of Al_2O_3–CeO_2 bidispersed suspensions. The stability behavior of these suspensions was investigated by sedimentation technique. It was concluded from this work that by increasing ceria nanoparticle concentration the stability of these bidispersed systems reaches an optimum condition, but further increasing of nanoparticles results in decreasing of the colloidal suspension stability. Also, the results showed that the suspensions have optimum dispersion state and high stability at pH 10. The calculated DLVO interparticle interaction potentials verified the experimental results of the pH effect on the stability behavior. The stabilization of the bidispersed suspensions was also evidenced by scanning electron microscopy (SEM) and SEM energy dispersive X-ray analysis (SEM/EDXA) of the sediment layers after 3 weeks.

Keywords: $A1_2O_3$; CeO_2; Stability; Suspensions; Nanoparticle

1. Introduction

Colloidal suspensions are being used increasingly in the consolidation of ceramic powders to produce green bodies. Compared to other methods such as dry or semidry state consolidation, colloidal methods can lead to better packing uniformity and better microstructural control during firing.[1]

The homogenization, dispersion and stabilization of ceramic particles in liquids are of primary importance for the preparation of highly performance ceramics through colloidal processing.[2] By tailoring interactions between colloidal particles, one can design stable suspensions. Attractive van der Waals forces must be balanced by repulsive interactions to engineer the desired degree of colloidal stability.[3]

Nanoparticle engineering is a novel method that may regulate the interaction between particles with high efficiency compared to conventional methods (such as modification of colloidal particle surfaces by polymeric dispersants[4–12] and surfactants[13–16]). This new stabilization mechanism was called "nanoparticle halos" mechanism, when proposed first by Tohver et al.[3] In this mechanism, high charged nanoparticles segregate to regions surrounding large colloidal particles, especially in systems with high size and charge difference, increase electrical surface charge of the matrix phase particles by halo formation around them and create more stable bidispersed suspensions.[3,17–20]

In "nanoparticle halos" mechanism, in addition to regulate the interparticle interactions, the inorganic nanoparticle hydrosol is considered as an efficient dispersant agent for ceramic powders, because it can not only provide high binding strength for ceramic bodies due to its conversion to a solid gel at relatively low temperature, but also improve the sinterability of ceramic powders.[2,21,22] But few studies have been conducted on the stabilization mechanism of this method. Also, the effect of different key variables such as the nanoparticles volume fraction and pH has been investigated in only a few especial bidispersed systems. Yao et al.[22] investigated the dispersion of talc particles in silica sol with different nanoparticle concentrations. Zhu et al.[2] studied the effect of silica nanoparticles on the stability of colloidal alumina particles. Fisher et al.[23] investigated the effect of silica nanoparticle size and concentration on

* Corresponding author. Tel.: +98 412 3443801; fax: +98 412 3224950.
E-mail address: a.babaluo@sut.ac.ir (A.A. Babaluo).

0955-2219/$ – see front matter © 2006 Elsevier Ltd. All rights reserved.
doi:10.1016/j.jeurceramsoc.2006.05.109

Table 1
Characteristics of materials

Materials	Function	Molecular formula	Characteristics	Supplier
α-Alumina	Matrix phase	α-Al_2O_3	Average particle size: 1 μm; average surface area: 6.55 m^2/g (Fig. 1)	Fibrona[a]
Ceria	Second phase	CeO_2	Average particle size: 30 nm (Fig. 1)	ANT[b]
Water	Dispersing media	H_2O	Deionized	Ghazi[c]

[a] Fibrona, 215 M. Shirazi Street, Tehran, Iran.
[b] Advanced Nano Technologies Pty Ltd., 112 Radium Street, Welshpool, WA 6106, Australia.
[c] Shahid Ghazi Pharmaceutical Co., Tabriz, Iran.

the stability of bidispersed alumina/silica suspensions. Their observation showed that in systems with high size difference, a lower content of nanoparticles is required to stabilize the bidispersed suspensions. Therefore, investigating the effects of these key variables in different bidispersed systems and finding suitable stabilization conditions, which would make it possible to predict experimental results, is necessary.

The aim of this research is to investigate the dispersion behavior and stabilization mechanism of alumina colloidal suspensions by highly charged ceria nanoparticles. The effect of ceria nanoparticle concentration on the stability of the colloidal alumina suspensions was investigated by a sedimentation method. The optimum weight fraction of the ceria nanoparticles was determined experimentally and compared with theoretical results obtained from "nanoparticle halos" theory. Also, pH effect on the stability of these bidispersed suspensions was studied and the results were verified by calculating the interparticle interaction potentials.

2. Experimental

2.1. Materials

The characteristics of the materials used in this work are given in Table 1 and also Fig. 1.

2.2. Suspension preparation

Bidispersed ceramic suspensions were prepared by adding the required weight fractions of alumina and ceria nanopowders in deionized water. Each slurry was stirred for about 24 h at 300-rotation per minute (rpm). The pH value of the slurries was adjusted by 0.1N NaOH or 0.1N HCl.

2.3. Sedimentation

The 5 wt.% alumina suspensions with different ceria contents ranging from 0 to 4.8 wt.% were prepared at pH 10. Also, to investigate the effect of pH, suspensions with 5 wt.% alumina particles and 3.84 wt.% ceria nanoparticles with different pH values ranging from 2 to 14 were prepared. The bidispersed suspensions were put in volumetric cylinders to measure the sedimentation volume as a function of time. The cylinders were capped to minimize solvent loss during the sedimentation experiment. The following information was reported for each sample: the height of the top interface that separates the supernatant (clear liquid) and cloudy liquid after 24 h and the sediment height after 3 weeks. For a good dispersion state, the following conditions should be obtained; the height of interface between clear and cloudy liquid after 24 h should be high, i.e. the powder should not have settled out of suspension in a short time, and the sediment height after 3 weeks should be low, i.e. the powder should pack very well when it does finally settle out of suspension.[14,24]

2.4. Characterization

Several methods were used for the characterization of the ceramic powders and sediment layers. The zeta potential of alumina and ceria particles dispersed in deionized water

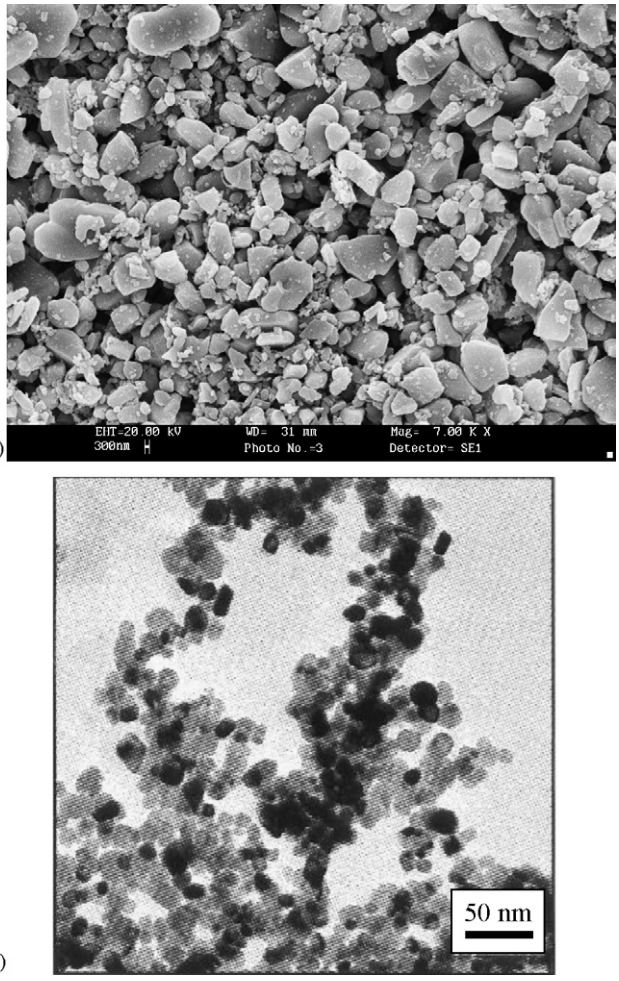

Fig. 1. (a) SEM micrograph of α-alumina powder and (b) TEM micrograph of ceria nanoparticles.

was measured with Zetasizer instrument (Zetasizer 3000 HS, Malvern, UK). The morphology of alumina powder and sediment layers was investigated with scanning electron microscopy (SEM, LEO 440I, 3×10^5, LEO, UK). Also, SEM energy dispersive X-ray analysis (SEM/EDXA) was used for the determination of the ceria nanoparticles distribution between the matrix phase particles in sediment layers.

3. Results and discussion

3.1. Zeta potential

The study of the electrokinetic behavior through measurement of the zeta potential becomes important for understanding the dispersion behavior of ceramic particles in a liquid medium. The zeta potential values of alumina and ceria suspensions at different pH values are presented in Fig. 2. According to the zeta potential values of alumina and ceria powders, pH 10 can be selected as an operating pH. Because, in this pH, both alumina and ceria particles have negative surface charge, $\xi_{Al_2O_3} = -18.2$ mV and $\xi_{CeO_2} = -31.2$ mV, respectively. Also this pH value is greater than the IEPs of alumina and ceria particles and ceria nanoparticles have high electrical surface charge compared to the matrix phase particles. Therefore, the "nanoparticle halos" mechanism can occur in these systems. But, for determining the exact operating pH, supplementary studies on the pH effect are necessary which are presented at Section 3.3.

3.2. Nanoparticles concentration effect

3.2.1. Sedimentation

Fig. 3 shows the height of the interface between clear and cloudy liquid after 24 h for 5 wt.% alumina suspension with different ceria nanoparticle concentrations at pH 10. With increasing ceria nanoparticle concentration, the cloudy height percent increases significantly and reaches a maximum of 96% at 3.84 wt.% ceria concentration. With further increase of ceria concentration, the suspension height decreases dramatically. When the ceria concentration reaches 4.8 wt.%, the cloudy height percent is about 86%. It indicates that ceria nanoparticles can enhance the dispersion of the alumina particles at pH

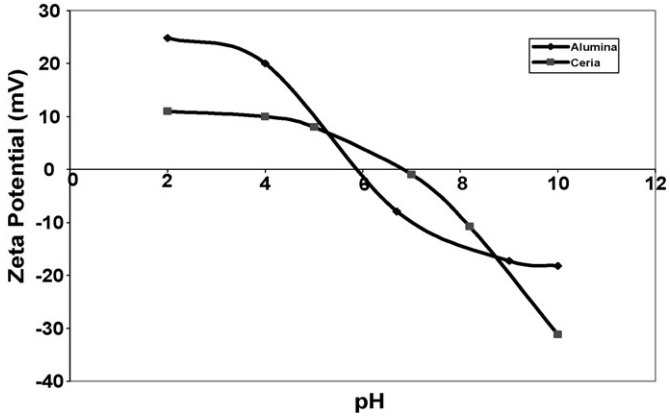

Fig. 2. Zeta potential as a function of pH for alumina and ceria particles.

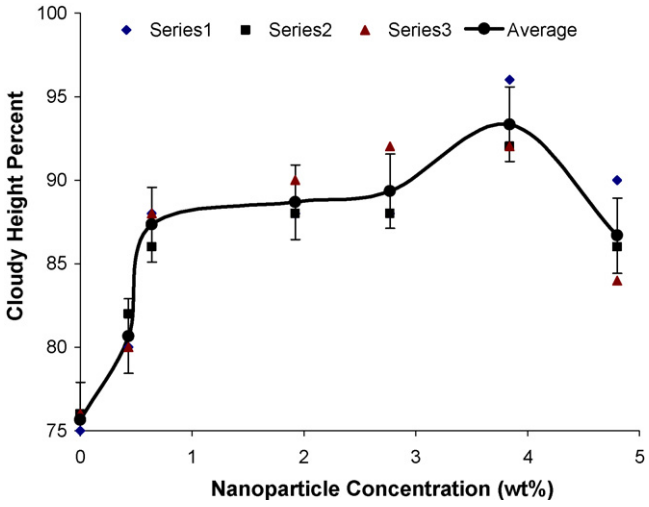

Fig. 3. Cloudy height percent as a function of nanoparticles concentration after 24 h.

10, and the ceria concentration corresponding to the optimum dispersion for 5 wt.% alumina slurry is around 3.84 wt.%.

The obtained results show that the stability of the alumina slurries depends significantly on the ceria nanoparticles concentration (cloudy height percent in the optimum nanoparticle

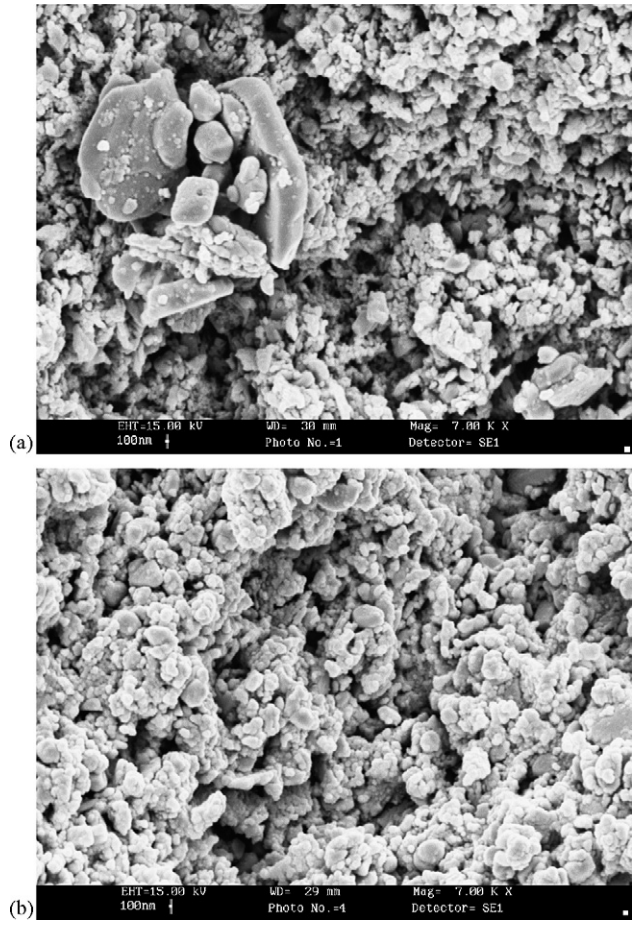

Fig. 4. SEM micrograph of sediments with: (a) $C_{nano} = 0.433$ wt.% and (b) $C_{nano} = 3.84$ wt.% ceria nanoparticle concentration.

concentration increases about 20% related to the pure alumina slurries). When the ceria concentration is very low, for example, as low as 0.433 wt.%, the monolayer halos could not form completely around the alumina particles. Therefore, the alumina particles form flocculated structures and settle rapidly, but these systems are more stable than the pure alumina slurries (see Fig. 3). When the ceria nanoparticle concentration was high enough, a monolayer halo of ceria nanoparticles forms around the alumina particles and stabilizes the resultant bidispersed suspension. By increasing the ceria concentration further, there are abundant ceria nanoparticles in the bulk liquid phase which result in increase of depletion attractive forces and instability of the slurry.[3,25–28] Also, in the higher ceria concentration, nanoparticles contact each other to form flocculated structures. It is therefore proposed that the dispersion and stabilization of alumina particles are attributed to the ceria nanoparticle halo formation around the alumina particles. The highly charged ceria nanoparticles are segregated to regions surrounding alumina particles. This segregation is driven solely by a Coulombic repulsion between ceria nanoparticles in solution and occurs because the alumina particles represent a big volume without big electrical surface charge. This type of haloing process can provide a mechanism for stabilizing colloidal species.

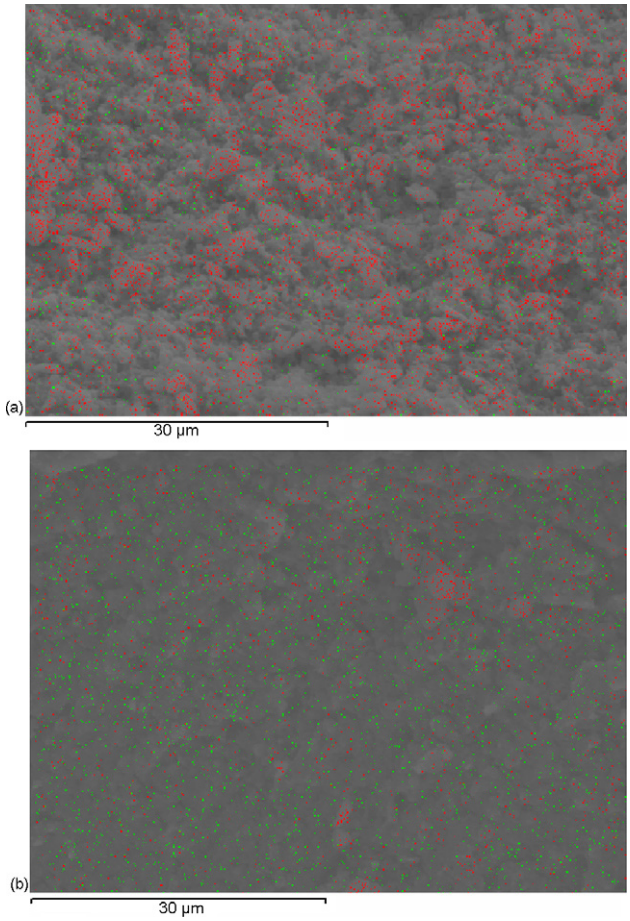

Fig. 5. SEM/EDXA results of sediments with: (a) $C_{nano} = 0.433$ wt.% and (b) $C_{nano} = 3.84$ wt.%; red dots: Al_2O_3 and green dots: CeO_2.

3.2.2. Morphology of sediment layers

Scanning electron microscope (SEM) images are taken to investigate the surface coverage of the alumina particles by the ceria nanoparticles and the distribution of alumina particles after sedimentation of the alumina/ceria bidispersed suspensions. Fig. 4 shows the SEM micrographs of the cross-sections of the sediment layers obtained from 5 wt.% alumina suspensions with 0.433 and 3.84 wt.% of ceria nanoparticle. At low concentration of ceria nanoparticle, the surface coverage of alumina particles is incomplete and the alumina particles tend to form flocculated structures. As the concentration of nanoparticles reaches its optimum value, the homogeneous microstructures are obtained by the formation of a complete nanoparticle halo around the alumina particles. SEM/EDXA results (dot-mapping) presented in Fig. 5, also show a good dispersion of the ceria nanoparticles in sediment layer cross-section at the optimum nanoparticle concentration. But, at low nanoparticle concentration the surface of the alumina particles has not been covered by the ceria nanoparticles, completely. These results prove the results obtained in prior sections.

3.3. Effect of pH

3.3.1. Sedimentation

The cloudy and sediment height of 5 wt.% alumina suspensions containing optimum weight percent of the ceria nanoparticles (3.84 wt.%) as a function of pH is shown in Fig. 6. The highest cloudy height occurred at pH 10, this indicates a good dispersion of alumina particles, which is attributed to charge

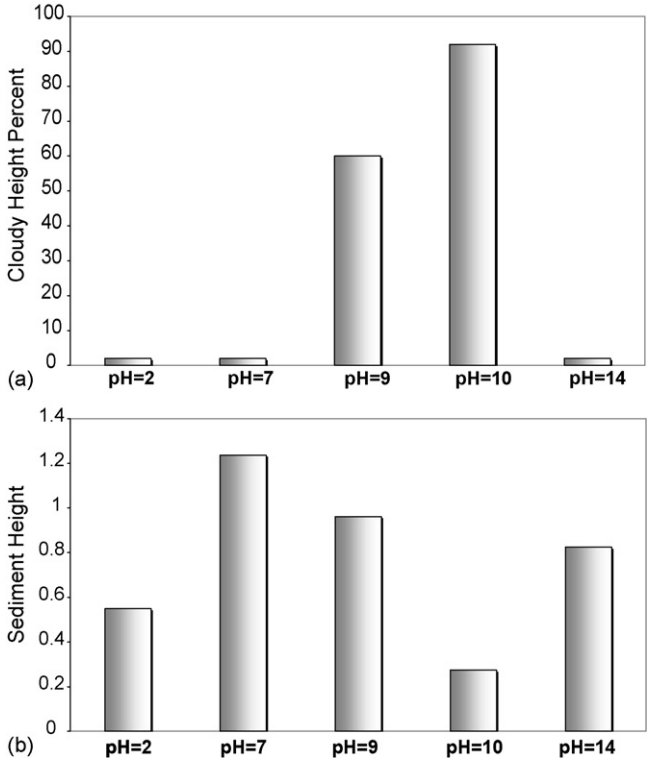

Fig. 6. (a) Cloudy height percent after 24 h and (b) sediment height (mm/1 wt.% powder) after 3 weeks as a function of pH.

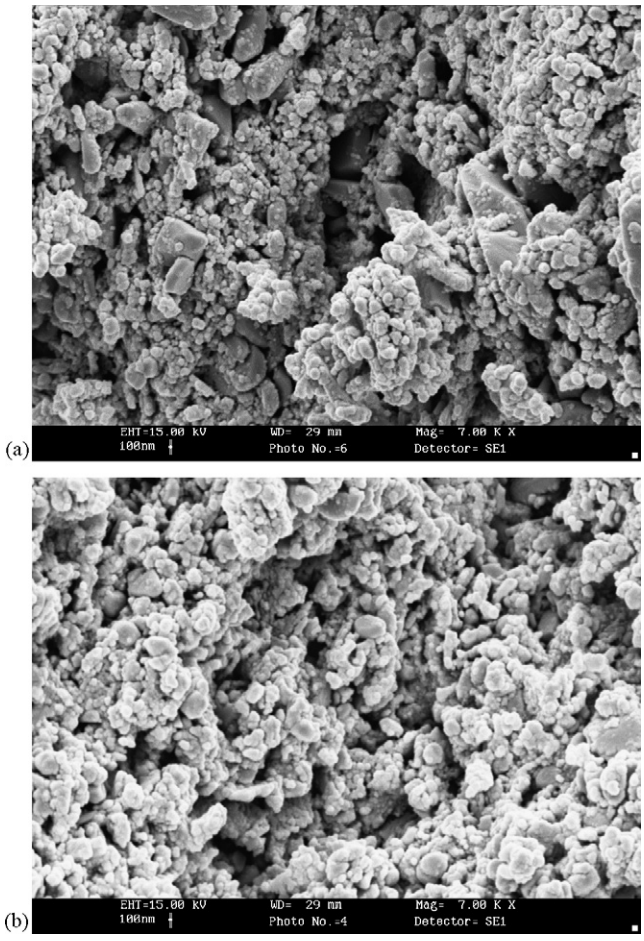

Fig. 7. SEM micrograph of sediments obtained from 5 wt.% alumina suspension with 3.84 wt.% nanoparticles at (a) pH 2 and (b) pH 10.

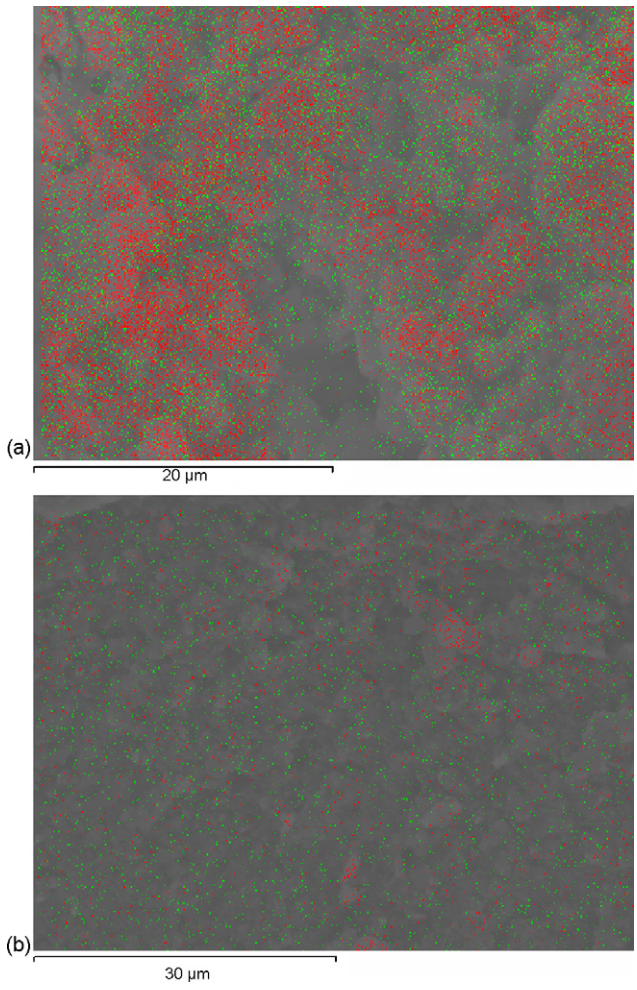

Fig. 8. SEM/EDXA results of sediments with C_{nano} = 3.84 wt.% at (a) pH 2 and (b) pH 10.

build up on the surface of alumina particles due to ceria nanoparticle haloing around them. Halo formation results in higher absolute zeta potential values of suspension. Therefore, the suspension in pH 10, is more stable compared to others which are far from this pH value. When the pH reaches the IEP region of alumina and ceria particles, the net surface charge of particles is zero and attractive van der Waals forces are dominant. In this condition, the uncharged particles attract each other and form agglomerated structures, which result in rapid sedimentation of particles and instability of bidispered suspension.

Variation of sediments height at different pH values is due to the different extents of agglomeration/dispersion of the particles which lead to different levels of particle packing in free space. The lower sediment height occurred at pH 10. This result is in good agreement with sedimentation tests at short time (after 24 h). The results indicate that the more stable suspensions result in sediments with high packing and low flocculated structures. Therefore, the sediment at pH 10 has an optimum packing compared to other samples (see Fig. 6b).

3.3.2. Morphology of sediment layers

Fig. 7 shows the scanning electron microscope (SEM) images of the cross-sections of the sediment layers obtained from 5 wt.% alumina and 3.84 wt.% ceria nanoparticles suspensions at pH 2 and 10. As shown in this figure, alumina particles tend to form flocculated structures in pH 2. In this pH, the absolute surface charge of alumina particles is greater than that of ceria nanoparticles; therefore, the halo formation around the alumina particles and the stabilization of the suspension by the halo mechanism is ineffective. At pH 10, increasing the electrical surface charge difference between ceria nanoparticles and alumina particles facilitates nanoparticle halo formation around the alumina microspheres and results in a homogenous structure with discrete alumina particles (see Fig. 7b). Also, as shown in Fig. 8, dot mapping of cerium and aluminum atoms in the sediment layers cross-section provides a uniform bidispersed microstructure at pH 10. But, at pH 2, no uniform distribution of the ceria and alumina particles is observed (see Fig. 8a).

3.4. Evaluation of the results

3.4.1. Optimum nanoparticles concentration

Kong et al.[1] have developed an equation for the calculation of optimum nanoparticle concentration based on the halo model. They have related the optimum weight fraction of nanoparticles (C_S) to volume fraction of microspheres (V_A), microspheres

weight in the suspension (W_A), density of microspheres (ρ_A) and density of nanoparticles sol (ρ_{sol}):

$$C_S = \frac{V_A}{1 - V_A} \frac{W_S}{W_A} \frac{\rho_A}{\rho_{sol}} \quad (1)$$

The W_S/W_A ratio arises from the following equation:

$$\frac{W_S}{W_A} = \frac{S_{WA} \pi r \rho_S}{4} \quad (2)$$

where W_S is the nanoparticle weight in the monolayer halos around the microspheres, S_{WA} the specific surface area of the microspheres and r is the average radius of the nanoparticles. The optimum ceria nanoparticle concentration according to Eqs. (1) and (2), is 2.77 wt.%, where $S_{WA} = 6550\ m^2/kg$, $r = 1.5 \times 10^{-8}$ m, $\rho_S = 6860\ kg/m^3$, $\rho_A = 3980\ kg/m^3$ and $\rho_{sol} \approx 1000\ kg/m^3$. As obtained before, the experimental ceria nanoparticle concentration for the best dispersion of the suspensions is 3.84 wt.%. The results show that the experimental ceria nanoparticle concentration corresponding to best dispersion is about 1.4 times that of the results obtained from Eqs. (1) and (2). The overall agreement between experimental and theoretical results is good and a monolayer halo of ceria nanoparticles is accordingly formed around the alumina microspheres. But, discrepancies between the results can be related to the existence of a certain amount of the ceria nanoparticles in the bulk solution.

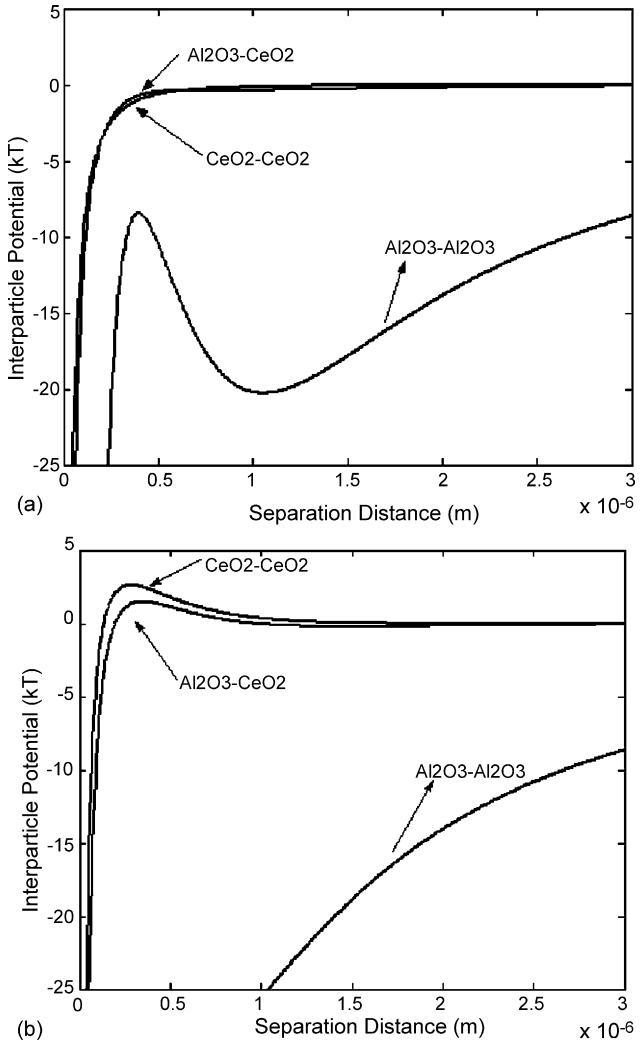

Fig. 9. The calculated DLVO interparticle interaction potentials between Al_2O_3–Al_2O_3, CeO_2–CeO_2 and Al_2O_3–CeO_2; (a) pH 2 and (b) pH 10.

3.4.2. Interparticle interaction potentials

The calculated DLVO interparticle interaction potentials[1] between Al_2O_3–Al_2O_3, CeO_2–CeO_2 and Al_2O_3–CeO_2 at pH 2 and 10 are shown in Fig. 9. The Hamaker constant of Al_2O_3 is 3.67×10^{-20} J.[29] The Hamaker constant of CeO_2 was calculated according to the single oscillator approximation (SOA) method[30] equal to 5.57×10^{-20} J. As shown in Fig. 9, in pH 2, the attractive van der Waals forces are dominant interparticle forces. This leads to formation of flocculated structures, which result in rapid settling of particles in these bidispersed suspensions. When the pH value reaches to 10, calculation indicate a net repulsive interaction between ceria and alumina particles, which is very close to that between ceria nanoparticles. The repulsion barrier between ceria nanoparticles and alumina particles hinders the adsorption of the ceria nanoparticles onto the surface of alumina particles and show that the ceria nanoparticles only segregated near the surface of alumina particles and form halos around them, which result in stable alumina-ceria bidispersed suspension.

4. Conclusion

Based on the work done in this research, the following general conclusions can be presented:

- *Nanoparticles weight fraction*. The stability behavior of the 5 wt.% alumina suspensions with different ceria contents ranging from 0 to 4.8 wt.% was investigated at pH 10 by sedimentation techniques. It was indicated that ceria nanoparticles can enhance the dispersion of the alumina particles at pH 10 by forming a monolayer halo around alumina particles. The ceria nanoparticles concentration corresponding to the optimum dispersion for 5 wt.% alumina slurry was determined around 3.84 wt.% experimentally, which was about 1.4 times the value obtained from theoretical equations. This discrepancy between the results can be related to the existence of a certain amount of the ceria nanoparticles in the bulk solution.
- *The effect of pH*. The effect of pH on the stability of the alumina-ceria bidispersed suspension was critical. At pH 10, a good dispersion of alumina particles was obtained which is attributed to charge build up on the surface of alumina particles due to high charged ceria nanoparticles haloing around them. The calculated DLVO interparticle interaction potentials verified the experimental results of the pH effect on the stability behavior of the investigated bidispersed suspensions.

Therefore, the high charged ceria nanoparticles halo formation around alumina particles and stabilization of suspension by halos mechanism was verified at pH 10 for 5 wt.% alumina microspheres and 3.84 wt.% ceria nanoparticles suspensions. These conclusions can be used in manufacturing nanocomposite microstructures, practically.

Acknowledgments

The authors wish to thank Sahand University of Technology (SUT) for the financial support of this work. Also, thank co-workers and technical staff in the research center for polymeric materials of SUT and Fibrona Company for their help during various stages of this work.

References

1. Kong, D., Yang, H., Yang, Y., Wei, S. and Cheng, B., Dispersion behavior and stabilization mechanism of alumina powders in silica sol. *Materials Letters*, 2004, **58**, 3503–3508.
2. Zhu, X., Jiang, D., Tan, S. and Zhang, Z., Dispersion properties of alumina powders in silica sol. *Journal of European Ceramic Society*, 2003, **21**, 2879–2885.
3. Tohver, V., Smay, J. E., Bream, A., Braun, P. V. and Lewis, J. A., Nanoparticle halos: a new colloidal stabilization mechanism. *Proceeding of the National Academy of Sciences of the United States of America*, 2001, **98**(16), 8950–8954.
4. Liufu, S., Xiao, H. and Li, Y., Adsorption of poly(acrylic acid) onto the surface of titanium dioxide and the colloidal stability of aqueous suspensions. *Journal of Colloids and Interface Science*, 2005, **281**, 155–163.
5. Shen, G. Z., Chen, F. J., Zou, K. H. and Yun, J., Dispersion of nanosized aqueous suspensions of barium titanate with ammonium polyacrylate. *Journal of Colloid and Interface Science*, 2004, **275**, 158–164.
6. Singh, B. P., Bhattacharjee, S., Besra, L. and Sengupta, D. K., Evaluation of dispersibility of aqueous alumina suspension in presence of darvan C. *Ceramics International*, 2004, **30**, 939–946.
7. Shi, C. Y., Wu, S. Y., Li, G. J. and Li, Z. G., Surface and rheology characterization of NH_4PAA-stabilized nanosized TiO_2 suspensions. *Journal of Dispersion Science and Technology*, 2003, **24**(5), 739–743.
8. Liu, Y., Gao, L. and Sun, J., Effect of acrylic copolymer adsorption on the colloidal stability of a 3Y-TZP suspension. *Journal of European Ceramic Society*, 2002, **22**, 863–871.
9. Blanco López, M. C., Rand, B. and Riley, F. L., Polymeric stabilisation of aqueous suspensions of barium titanate. Part I: effect of pH. *Journal of European Ceramic Society*, 2000, **20**, 1579–1586.
10. Santhiya, D., Subramanian, S., Natarajan, K. A. and Malghan, S. G., Surface chemical studies on alumina suspensions using ammonium poly(methacrylate). *Colloid and Surfaces A: Physicochemical and Engineering Aspects*, 2000, **164**, 143–154.
11. Davis, J. and Binner, J. G. P., The role of ammonium polyacrylate in dispersing concentrated alumina suspensions. *Journal of European Ceramic Society*, 2000, **20**, 1539–1553.
12. Blanco López, M. C., Rand, B. and Riley, F. L., Polymeric stabilisation of aqueous suspensions of barium titanate, Part II: effect of polyelectrolyte concentration. *Journal of European Ceramic Society*, 2000, **20**, 1587–1594.
13. Popa, A. M., Vleugels, J., Verment, J. and Van der Biest, O., Influence of surfactant addition sequence on the suspension properties and electrophoretic deposition behavior of alumina and zirconia. *Journal of European Ceramic Society*, 2006, **26**, 933–939.
14. Tseng, W. J. and Teng, K. H., The effect of surfactant adsorption on sedimentation behaviors of Al_2O_3–toluene suspensions. *Materials Science and Engineering A*, 2001, **318**, 102–110.
15. Tseng, W. J., Influence of surfactant on rheological behaviors of injection-molded alumina suspensions. *Materials Science and Engineering A*, 2000, **289**, 116–122.
16. Terpstra, K. A., Pex, P. P. A. C. and Vries, A. H., *Ceramic Processing*. Chapman-Hall, UK, 1995.
17. Tohver, V., Chan, A., Sakurada, O. and Lewis, J. A., Nanoparticle engineering of complex fluid behavior. *Langmuir*, 2001, **17**, 8414–8421.
18. Martinez, C. J., Liu, J., Rhodes, S., Luijten, E., Weeks, E. R. and Lewis, J. A., Interparticle interactions and direct imaging of colloidal phases assembled from microsphere-nanoparticle mixtures. *Langmuir*, 2005, **21**(22), 9978–9989.
19. Liu, J. and Luijten, E., Stabilization of colloidal suspensions by means of highly charged nanoparticles. *Physical Review Letters*, 2004, **93**, 248303.
20. Karanikas, S. and Louis, A. A., Dynamic colloidal stabilization by nanoparticle halos. *Physical Review Letters*, 2004, **93**, 247802.
21. Yang, Q. and Troczynski, T., Dispersion of alumina and silicon carbide powders in alumina sol. *Journal of American Ceramics Society*, 1999, **82**, 833–840.
22. Yao, X., Tan, S., Huang, Z. and Jiang, D., Dispersion of talc particles in silica sol. *Materials Letters*, 2005, **59**, 100–104.
23. Fisher, M. L., Colic, M., Rao, M. P. and Lange, F. F., Effect of silica nanoparticle size on the stability of alumina/silica suspensions. *Journal of American Ceramics Society*, 2000, **84**(4), 713–718.
24. Janney, M. A., Omatete, O. O., Walls, C. A., Nunn, S. D., Ogle, R. J. and Estmoreland, G., Development of low toxicity gel-casting system. *Journal of American Ceramics Society*, 1998, **81**(3), 581–591.
25. Kristoffersson, A., Lapasin, R. and Galassi, C., Study of interaction between polyelectrolyte dispersant, alumina and latex binder by rheological characterisation. *Journal of European Ceramic Society*, 1998, **18**, 2133–2140.
26. Xu, W., Nikolov, A. D. and Wasan, D. T., Role of depletion and surface induced structural forces in bidispersed suspensions. *AIChE Journal*, 1997, **43**(12), 3215–3222.
27. Walz, J. Y. and Sharma, A., Effect of long range interaction on the depletion force between colloidal particles. *Journal of Colloid and Interface Science*, 1994, **168**, 485–496.
28. Mao, Y., Cates, M. E. and Lekkerkerker, H. N. W., Depletion force in colloidal systems. *Physica A*, 1995, **222**, 10–24.
29. Bergström, L., Hamaker constant of inorganic materials. *Advances in Colloid and Interface Science*, 1997, **70**, 125–169.
30. French, R. H., Origins and application of London dispersion forces and Hamaker constants in ceramics. *Journal of American Ceramics Society*, 2000, **83**(9), 2117–2146.